# Mathematical Modeling of Tin-Free Chemically-Active Antifouling Paint Behavior

**Diego Meseguer Yebra, Søren Kiil, and Kim Dam-Johansen**
Dept. of Chemical Engineering, Technical University of Denmark, Lyngby, Denmark

**Claus E. Weinell**
Hempel A/S, Lyngby, Denmark

*DOI 10.1002/aic.10787*
*Published online February 15, 2006 in Wiley InterScience (www.interscience.wiley.com).*

*Mathematical modeling has been used to characterize and validate the working mechanisms of tin-free, chemically-active antifouling (AF) paints. The model-based analysis of performance data from lab-scale rotary experiments has shown significant differences between antifouling technologies as regards the biocide leaching and the surface polishing processes. Hence, the modeling framework developed in this work is built so as to describe any generic, chemically-active AF paint through model parameters, the values of which can be obtained or adjusted from relatively fast measurements. The detailed quantitative information on reacting AF paint systems obtained can be used for accelerated product optimization purposes, thus facilitating the transition to cleaner antifouling technologies using, for example, fast-degrading natural or synthetic bioactive components.*© 2006 American Institute of Chemical Engineers *AIChE J,* 52: 1926–1940, 2006
*Keywords: mathematical modeling, controlled release formulations, tin-free antifouling paints, biocide release rate, chemical product design*

## Introduction

The problems associated with the fouling of artificial surfaces by marine organisms have been acknowledged since ancient times.[1–4] The organisms, which take part in the process of marine biofouling, are primarily the attached (or sessile) forms that occur naturally in the shallower water along the coast.[1] The latter reference reported that nearly 2,000 species had been identified on fouled structures; another source has increased the number to more than 4,000 species.[5] During the 1990s, the use of effective antifouling (AF) protection, allowing extended dry-docking intervals on ocean-going ships, rendered estimated savings as high as $5.7 billion annually worldwide[6] and fuel savings on the order of 7 million tons per year.[7] Until now, such an effective and long-lasting protection has only been achieved by means of chemically active antifouling paints. Among them, the tributyltin self-polishing copolymer (TBT-SPC) technology was the first one to yield outstanding performances attributed to the so-called "self-polishing" behavior, which has traditionally been characterized by[4]:

- Sufficiently thin and stable leached layers, resulting in efficient and relatively constant biocide release rates over time;
- A polishing mechanism that allows satisfactory AF performance during stationary periods and permits long active lifetimes even at high sailing speeds;
- Smooth, practically fouling-free paint surfaces during sailing.[8,9]

Regarding the last point, potential variations in the microroughness among different self-polishing (SP) coatings were found not to involve a significant increase in the drag resistance of the vessel compared to large scale surface irregularities that result from, for example, shipbuilding, dry-docking activities, or macrofouling.[10]

This article includes Supplementary Material available from the authors upon request or via the Internet at http://www.interscience.wiley.com/jpages/0001-1541/suppmat/.

Current address for D. M. Yebra is Pinturas Hempel, Carretera de Sentmenat 108, E-08213, Polinyà, Barcelona, Spain.
Correspondence concerning this article should be addressed to S. Kiil at sk@kt.dtu.dk.

### *The transition to tin-free coatings*

The first legal measures against the TBT-SPC technology, which was used at that time by as much as 70% of the world fleet of ocean-going ships,[11,12] shook the AF paint industry. The tin-containing moieties were found not to degrade sufficiently fast in seawater, causing a series of sublethal effects on a number of non-target marine organisms.[4,13,14] Marine paint companies were forced to develop products providing the same AF efficiency, but based on substances with a better environmental profile. Just to give an idea of how difficult that challenge was, several authors claimed in the late 1990s (that is, after more than a decade of intense tin-free research) that organotins should be used until really effective alternatives were found.[7,15-17] The latter statement was mainly based upon the significant environmental benefits resulting from the lower fuel consumptions associated with clean ship hulls.

During the tin-free era, a large amount of research has also been focused towards the development of non-toxic technologies based on different antifouling mechanisms, such as the non-stick and, more importantly, the fouling release approaches.[14,18] The advances in the race to liberate the oceans from the extensive use of biocides are notorious, and several silicon-based commercial products are already available for high-activity high-speed vessels and propellers.[4,18] Nevertheless, there are still many important hurdles that should be overcome for a widespread use by all the fleet of ocean-going vessels.[4]

A second group of alternatives is based on the deterrent properties of some extracts obtained from marine organisms. Even for those natural compounds based on a toxic mode of action (see other reported mechanisms[4,19]), their natural origin might assure an effective biodegradation and satisfactory environmental profile.[4,20,21] Unfortunately, the commercial large-scale implementation of this technology seems far away in time, as it requires not only the identification of the proper active compound(s), but also:

- A successful incorporation into paint systems (i.e., stability);
- A controlled release of these substances (i.e., active concentrations at the paint surface[22]) so that a long lasting fouling protection is attained;
- Long and costly registration process of the active component[19];
- Large scale production at competitive prices.

Despite the increasing interest in these promising emerging technologies, the best wide-spectrum AF protection in the post-tin era is still associated with chemically-active AF paints based on the release of $Cu^{2+}$ and synthetic co-biocides (algaecides).

*Current Design and Optimization Procedures.* The eminently empirical approach (such as long-term rotary experiments and raft testing) used by the paint companies involved a slow transition to efficient controlled-release tin-free products. As an example, the time-consuming optimization process of one of the main current tin-free acrylic-based SP technologies (based on a copper acrylate resin), which led to different European patents in the period from 1986 to 2001, is described elsewhere.[4] In 1997, that is, 11 years after the first European patent, such a technology was only available for coastal vessels with up to 3 years of drydocking interval.[23] The lower efficiency of the tin-free products compared to the TBT-SPCs meant that the major antifouling paint companies (that is, International Marine Coatings, Hempel A/S, Jotun, Ameron International, Chugoku Marine Paints) decided to remove tin-based coatings from their product assortment only a few months before the suggested date for the ban on the application of these products (1 January, 2003).

*Future Changes in AF Coatings.* Recent reviews[24,25] claim that most of the currently used co-biocides do accumulate in the environment in sufficient concentrations to cause sublethal effects on non-target organisms. Voulvoulis et al.[26] and, more recently, Katranitsas et al.[27] also expressed their doubts about the environmental effects of too large copper loads into the marine environment, the release rates of which will probably be restricted in the near future.[19] In the light of potential future regulations, novel and improved paint development procedures are necessary to assure that the transition to as efficient but, at the same time, more environmentally friendly coatings does not require another 15 years.

*Paint Modeling.* It is believed that the optimization of chemically-active AF products, or the design of new and improved ones, would be strongly eased if detailed kinetic studies on the different processes determining the paint activity were performed and combined.[22,28-31] The main difficulty in developing efficient AF products is that the coupling of the main paint processes is so marked that typically only very few formulations among a large number of possibilities result in adequate paint polishing and biocide leaching simultaneously. The substitution of one major paint component may cause a dramatic misbalance in the performance, which often takes years of research and development to solve.

The idea behind the modeling approach is to identify and characterize the main processes taking part in the AF paint performance. When such processes are quantified, the information acquired can subsequently be used as input to a mathematical model, which will eventually simulate the entire lifetime of any paint composition (at least combinations of the main ingredients) at any seawater condition in just a few minutes time. If the resulting performance is not satisfactory, such a tool would be very helpful in isolating and diagnosing the weak points of a technology and, subsequently, in driving the screening process for a successful replacement. Additionally, paint models are useful "learning tools," which can help antifouling paint producers in a more scientific approach to paint design and formulation.

*Experimental Performance of Antifouling Model Paints.* In order to validate the model to be presented in the following section and to estimate certain model parameters, a set of ablative, rosin-based antifouling model formulations were prepared and subjected to rotary testing in artificial seawater at controlled shear stress conditions[32] (see Table 1). The rotary rig consists of a 0.5 $m^3$ artificial seawater tank in which a rotating cylinder, with the paints attached to its outer surface, is immersed. Such a cylinder is surrounded by a wall placed at a few centimeters distance, aiming at approaching Couette flow (constant shear stress) for the water in the narrow channel. The experimental AF model paint performance results, together with an exhaustive description of the experimental rig and the experimental methods used, are available in [10,28,32]. The paints tested cover a wide range of formulation parameters, such as seawater soluble (such as $Cu_2O$, ZnO) and insoluble (such as, $Fe_2O_3$, $TiO_2$) pigment type, pigment volume concentration

**Table 1. Model AF Paint Formulations Containing $Cu_2O$ and Insoluble Pigment Particles Modeled in This Work***

| | Paint | | | | | |
|---|---|---|---|---|---|---|
| | Ti-1 | Ti-2 | Ti-3 | Ti-4 | Ti-5 | Fe-1 |
| ZnR | 73.3 | 73.3 | 73.3 | 73.3 | 50.5 | 73.3 |
| Hydrophobic 1 | 8.3 | 8.3 | 8.3 | 8.3 | — | 8.3 |
| Hydrophobic 2 | — | — | — | — | — | — |
| Hydrophobic 3 | — | — | — | — | 40.3 | 0.0 |
| Plasticizer 1 | 18.3 | 18.3 | 18.3 | 18.3 | 9.2 | 18.3 |
| Plasticizer 2 | — | — | — | — | — | — |
| Total | 100.0 | 100.0 | 100.0 | 100.0 | 100.0 | 100.0 |
| $Cu_2O$ | 15.0 | 20.0 | 25.0 | 20 | 20.0 | 15.0 |
| $TiO_2$ | 15.0 | 20.0 | 20.0 | 10 | 20.0 | — |
| $Fe_2O_3$ | — | — | — | — | — | 15.0 |
| Fibers | 5.0 | 5.0 | 5.0 | 5.0 | 0.0 | 5.0 |
| PVC | 35.0 | 45.0 | 50.0 | 35.0 | 40.0 | 35.0 |

*The binder compositions are given in solids volume percent of binder (note that the ratio ZnR/plasticizer remains constant but in Ti-5). The pigment PVC is given in solids volume percent. The paint names are the same as in Yebra et al.[32]

(PVC) and particle size distribution (PSD), and various binder compositions and ratios.

## The Mathematical Model

The model presented in this work is based on that developed by Kiil et al.[28] for tin-based paints, but extended here so as to describe any generic chemically-active AF paint through adjustable parameters. The reason for this was that some of the a priori mechanistic assumptions underlying the TBT-SPC model were found not to apply to other modern AF technologies. The latter was most evident when modeling simple AF formulations incorporating large amounts of a rosin-based binder of wide commercial interest (to be presented in this article). Most of the currently commercialized tin-free acrylate-based resins need to use rosin or rosin-derivatives in order to adjust the intrinsic hydrophobicity and erosion resistance of the coating to the levels yielding the desired polishing rate.[4] A second group of paints uses rosin-derivatives as the main reactive binder, while co-binders and reinforcing mineral microfibers can be used to provide the required resistance to water penetration and appropriate mechanical properties.[4]

The main seawater reactive resin in the binder considered in this work is a synthetic substitute of natural rosin (subject to hydrogenation and distillation) that has been claimed to be more consistent and less sensitive to oxidation (lower number of double bonds), while retaining a suitable seawater solubility.[4,33] This rosin derivative is further reacted to form zinc carboxylate (which is sometimes called zinc resinate), which gives rise to the controlled-polishing properties through an alkaline hydrolysis reaction. The zinc derivative entails an increased hardness and faster drying times compared to the hydrogenated rosin. The most likely overall reaction mechanism was presented in Yebra et al.[33] and can be summarized by the following expression:

$$\underset{\text{ZnR (insoluble)}}{RCOO-Zn-OOCR(s)} + 2Na^+ \rightleftarrows \underset{\text{Soluble residues}}{2RCOO^-Na^+(aq)} + Zn^{2+} \qquad \text{(Reaction 1)}$$

The natural origin of the resin and its relative hydrophilicity might involve a better compatibility with future antifoulants of natural origin than strongly hydrophobic synthetic polymeric binders.[4,19] In this sense, it is very important that the active compound is distributed homogeneously in the dry binder without any significant chemical degradation, which might endanger its AF activity. Finally, the low price, wide availability, and extensive experience accumulated on rosin-based product development are some of the reasons why this binder has been chosen for this study. The co-binders used in this investigation are similar to those used in short specification time, ablative AF formulations.

### *Problem description*

A thorough description of the physical and chemical system to be modeled is provided next (see Figure 1). Seawater ions are transported to the paint surface by diffusion through a laminar boundary layer developed at the paint surface. There, $Cl^-$- and $H^+$-ions react with the $Cu_2O$ surface exposed, leading to the formation of chloro-copper complexes ($CuCl_2^-$ and $CuCl_3^{2-}$). These complexes are oxidized to $Cu^{2+}$-species during the transport of these complexes away from the pigment surface and potentially accumulated in the slimes formed on the paint surface[34,35] where the oxidation process is probably completed. The resulting concentration level of biocidal species at the paint surface is responsible for a toxic effect on animal fouling species mainly. The $Cu_2O$ dissolution reactions can be written as follows[28,36]:

$$\tfrac{1}{2}\,Cu_2O(s) + H^+ + 2Cl^- \leftrightarrows CuCl_2^- + \tfrac{1}{2}\,H_2O(1) \qquad \text{(Reaction 2)}$$

$$CuCl_2^- + Cl^- \leftrightarrows CuCl_3^{2-} \qquad \text{(Reaction 3)}$$

Reaction 2 is reversible and influenced by kinetics, whereas Reaction 3 is reversible and instantaneous and can be considered in equilibrium at all times. The oxidation reaction leading to $Cu^{2+}$ is presented under the model development section.

When the uppermost pigment layer has been dissolved, water molecules permeate through the binder membrane separating two $Cu_2O$ particles and start dissolving the underlying pigment layer. Consequently, a highly concentrated copper solution builds up under the membrane, resulting in an osmotic disequilibrium that leads to membrane breakage, thus exposing the unreacted pigment particle.[37] There is no detailed information in the literature about the characteristics of the leached structure left after the removal of the interparticle binder membrane and its dependence on, e.g., the mechanical properties of the binder. However, we hypothesize that the differences in the mechanical properties between the TBT-SPC polymers and the tin-free model binder are responsible for major differences in the pore morphology and, hence, on the AF paint behavior (see discussion later on).

The continuous removal of copper from the solid pigment phase creates voids in the uppermost paint layer, so seawater ions must penetrate into these voids to reach the dissolving pigment surface. The distance from this dissolving front to the paint surface is termed the "leached layer," which can be described as a porous, soluble pigment-depleted, binder matrix

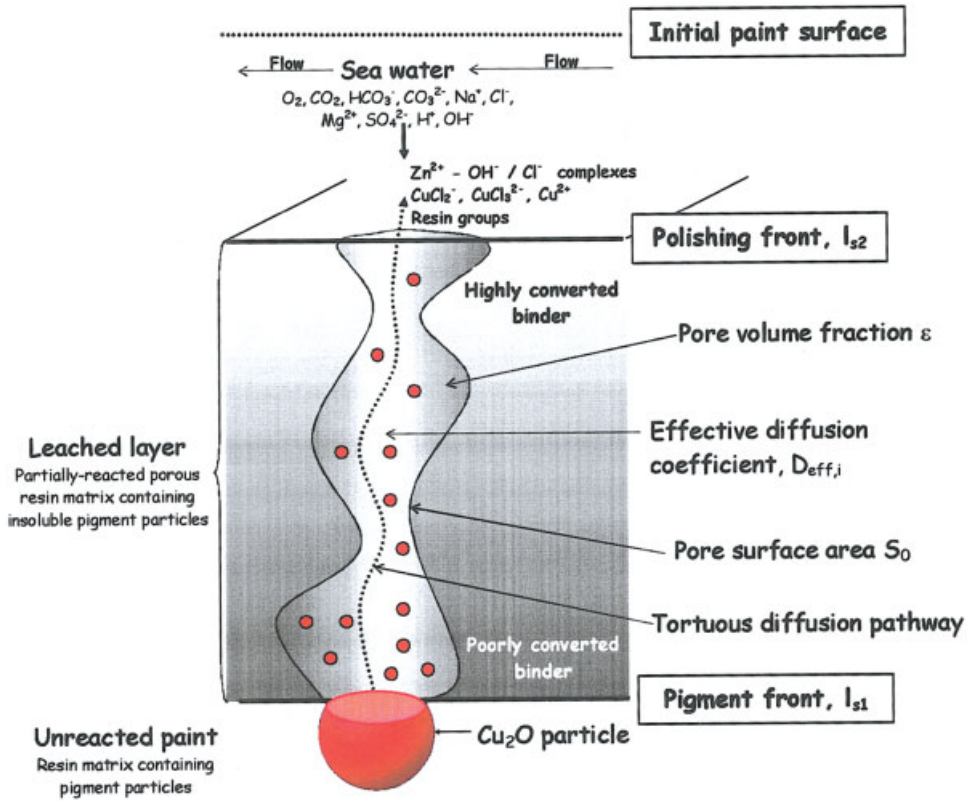


**Figure 1. Paint surface pore created by dissolution of $Cu_2O$ pigments.**

Some modeling concepts are also included. [Color figure can be viewed in the online issue, which is available at www.interscience.wiley.com.]

(see Figure 1). The fact that some binder components are susceptible to seawater reaction (see, for example, Reaction 1) means that the pore walls are also exposed to chemical attack. At a certain point in time, the binder close to the paint surface will show a high degree of conversion, as it has been exposed for a relatively long period of time. On the contrary, at the pigment front, the binder matrix surrounding the pigments is being slowly uncovered by the dissolution of the pigment particle, thus having virtually the same chemical composition as the unreacted binder. As a result of the chemical degradation of the binder, its resistance to erosion diminishes.

Summarizing, the activity of chemically-active AF paints can be properly inferred from the modeling of these core processes:

- The dissolution of the seawater pigments (such as $Cu_2O$, ZnO[38]) in seawater;
- The reaction of the active binder components with seawater;
- Surface polishing;
- Effective diffusion of chemical species in the leached layer;
- Chemical speciation calculations.

### *Model assumptions*

The assumptions made in the model presented in Kiil et al.[28] are basically kept for the tin-free rosin-based paint model, with the following additions/modifications:

*i. Binder Reaction.* The dissolution of the ZnR takes place throughout the leached layer, yielding the sodium salt of the hydrogenated rosin (HR) as the only stable dissolved product (see kinetics[33]).

*ii. Binder Composition.* From the total amount of ZnR added to the paint, $4\%_{sv}$ is assumed to be converted to $Cu^{2+}$-resinate as a result of ion exchange during paint dispersion.[33] The binder components are assumed to be homogeneously distributed throughout the paint film.

*iii.* $Cu_2O$ *Dissolution Mechanism.* The TBT-SPC copolymer was assumed to be so hydrophobic that no water could diffuse through the binder beyond the pigment front. Thus, only the small uppermost portion of the pigment particles was exposed to seawater, and the chemical reaction (see Reaction 2) was the rate limiting process determining the release of aqueous Cu(I) species. Such an assumption led to concentrations of chloro-copper complexes at the pigment front far away from the equilibrium values. However, such an assumption was not regarded as valid for the modeling of the copper leaching from insoluble matrix paints[37,39,40] and saturation at the pigment front was assumed instead. For the paints studied here, the assumption of Cu(I) saturation at the pigment front is supported by the relatively significant water penetration characteristic of rosin-based products,[41,42] potentially leading to long contact times between $Cu_2O$ particles and seawater prior to exposure at the pigment front. Furthermore, and in good agreement with the latter discussion, the use of relatively hydrophilic plasticizers (such as Plasticizer 2[33]) has been shown to boost the copper leaching process.[43]

*iv.* Cu(I) *Oxidation.* The Cu(I) species (neglecting $Cu^+$, CuCl, and $CuCl_4^{3-}$ mentioned by Sharma and Millero[44]) are

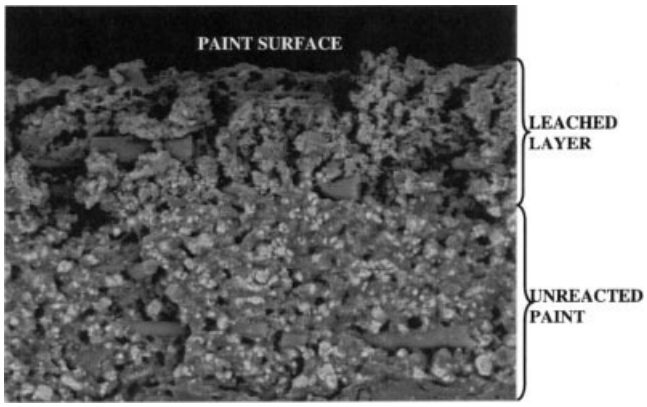


**Figure 2. SEM picture of an AF paint formulated with ZnR and exposed to the rotary setup for three months at 25°C and pH 8.2.**

Relatively open pores can be appreciated in the leached layer.

oxidized in the leached layer according to the kinetic expression presented in that same source.[44] The influence of the concentration of $HCO_3^-$, $Mg^{2+}$, and $Cl^-$ on the reaction rate is considered (see Supplementary Material). The stoichiometry of this redox reaction is proposed as follows[45,46]:

$$4Cu^+ + O_2 + 4H^+ \rightarrow 4Cu^{2+} + 2H_2O \quad \text{(Reaction 4)}$$

*v. Leached Layer Porosity.* Unlike in the TBT-SPC model, the walls of the polymer matrix are not stable over time as the result of the volume loss associated with the ZnR dissolution. The latter involves an increase of the pore size and a subsequent variation of the pore wall surface area over time.

*vi. Leached Layer Tortuosity Factor.* This parameter accounts for the ratio between the length of the actual tortuous pore path and the leached layer thickness. In the TBT-SPC model,[28] the value of the tortuosity factor was estimated through the simple empirical equation from Wakao and Smith[47]:

$$\tau_1(t) = \frac{1}{\varepsilon_1(t)} \tag{1}$$

In the present study, in which insoluble pigments are also used, the value of the tortuosity factor is determined through the modeling of the experimental leaching process (see the Results and Discussion section). The values of the tortuosity factor that are used in the description of the leaching process in the tin-free model paints studied in this work are sensibly lower than those that would result from [4], which means that "bottle neck" structures (see schematic drawings[48]) are not formed extensively as a result of the $Cu_2O$ dissolution process (Figure 2). In the tin-free model, the tortuosity factor of the pores is also assumed to develop (diminish) with time as a consequence of the pore broadening process resulting from the reaction at the walls.

*vii. Leached Layer Surface Area.* In order to model the change in the binder surface exposed during immersion, the pores are assumed to develop a conical geometry after a sufficient exposure time from an initial somewhat cylindrical shape.[48] This assumption involves that the loss of active binder takes place homogeneously at the pore walls, neglecting the presence of insoluble ingredients.

In the TBT-SPC model,[28] the pores developed in the leached layer were assumed to have a surface area equal to the external surface area of the $Cu_2O$ pigments (see Yebra[48] for a better understanding of the assumption). It is believed that the pore structure resulting from the use of weaker binder systems will be broader. Even though the use of reinforcing microfibers has been demonstrated to markedly improve the macroscopic mechanical properties of the paint film,[4] it seems evident that it cannot affect the binder properties at the microscale. Thus, we hypothesize that the fiber-free binder membrane separating the pigment particles exerts less resistance to the osmotic stresses associated with the pigment dissolution process,[37] resulting in relatively open pores of low tortuosity. The latter is further supported by the risk of development of brittle unplasticized binder areas upon exposure resulting from the leaching of hydrophilic plasticizers (such as Plasticizer 2[33,48]). Thus, an assumption of cylindrical pores is preferred, although a factor correcting for non-smooth pore wall surface, resulting from the irregular pigment particle shape, needs to be introduced. Also, the leaching of the soluble plasticizer should increase the ZnR exposed surface area.

*viii. Pore Wall Composition.* The assumption of stable pore walls led to a TBT-hydrolysis rate equation diminishing linearly with increasing values of polymer conversion.[28] In the rosin-based case, the molecules reacted are assumed to diffuse out into the bulk seawater, leaving a fresh binder layer behind.

### *New equations in the AF paint mathematical model*

*Leached Layer Porosity.* The evolution of the leached layer porosity value with time can be described through:

$$\varepsilon_1(t) = \varepsilon_0 + X_{\mathrm{ZnR}}(t)\big|_1 \cdot V_b \cdot f_{\mathrm{ZnR}} \tag{2}$$

This dynamic process reaches a pseudo steady-state provided that a constant conversion at the paint surface for a given set of exposure conditions is assumed after an initial lag-time ($X_{max}$ concept[28]).

*Leached Layer Tortuosity Factor.* The change in the value of the tortuosity factor as a result of the binder reaction is calculated as if Eq. 1 had been used to calculate the initial tortuosity factor:

$$\tau_1(t) = \tau_0 \cdot \frac{\varepsilon_0}{\varepsilon_1(t)} \text{ with } \tau_0 \cdot \varepsilon_0 \neq 1 \text{ (i.e. equation (1) is not used initially)} \tag{3}$$

Just like in the TBT-SPC model,[28] the effective diffusion coefficient is calculated through:

$$D_{e,i} = D_{\mathrm{water},i} \cdot \frac{\varepsilon}{\tau} \tag{4}$$

The effective diffusion coefficients are also modified in order to account for the change in the void volume of the leached layer:

$$D_{e,i}(t)\big|_1 = D_{\text{wat},i}\cdot\frac{\varepsilon_1(t)}{\tau_1(t)} = D_{\text{wat},i}\cdot\frac{\varepsilon_1(t)}{\tau_0\cdot\dfrac{\varepsilon_0}{\varepsilon_1(t)}} = D_{\text{wat},i}\cdot\frac{\varepsilon_0}{\tau_0}\cdot\frac{\varepsilon_1(t)^2}{\varepsilon_0^2}$$

$$= D_{e,i0}\cdot\frac{\varepsilon_1(t)^2}{\varepsilon_0^2} \quad (5)$$

The use of low values for the tortuosity factor is in good agreement with the pore morphology assumption to be presented in the next paragraph.

*Leached Layer Surface Area.* Just as in the TBT-SPC model,[28] the fraction of the paint surface initially occupied by the soluble pigments, assuming a perfect distribution, is equal to their Pigment Volume Concentration (PVC). Thus, the number of pores per unit of paint surface would be

$$N_{\text{pore}} = \frac{f_{\text{Cu}_2\text{O}}}{\bar{S}_{\text{Cu}_2\text{O}}} = \frac{f_{\text{Cu}_2\text{O}}}{2/3\cdot\pi\cdot(\bar{d}_{\text{Cu}_2\text{O}}/2)^2} = \frac{6\cdot f_{\text{Cu}_2\text{O}}}{\pi\cdot\bar{d}^2_{\text{Cu}_2\text{O}}} \quad (6)$$

where

$$\bar{S}_{\text{Cu}_2\text{O}} = \frac{2\cdot\pi}{3}\cdot\bar{r}^2_{\text{Cu}_2\text{O}} \quad (7)$$

and

$$\bar{r}_{\text{Cu}_2\text{O}} = \sum_{i=1}^{N}\phi_i\cdot r_{\text{Cu}_2\text{O}_i} \quad (8)$$

In Eq. 8, the mean particle diameter ( $\bar{r}_{\text{Cu}_2\text{O}}$) is obtained from Laser Diffraction Particles Size Distribution (PSD) measurements.[28,32] The exposed binder surface at the pore walls, assuming a completely leached paint film and tortuous pores, is calculated under the assumption of cylindrical pores:

$$S_{\text{pores}} = N_{\text{pores}}\cdot(L_p\cdot\tau)\cdot\left(2\cdot\pi\cdot\left(\frac{2}{3}\right)^{1/2}\cdot\bar{r}_{\text{Cu}_2\text{O}}\right) \quad (9)$$

The value of the total exposed pore surface per unit paint volume can be calculated by:

$$S_{0_{\text{cyl}}} = N_{\text{pores}}\cdot\tau\cdot\left(2\cdot\pi\cdot\left(\frac{2}{3}\right)^{1/2}\cdot\bar{r}_{\text{Cu}_2\text{O}}\right) \quad (10)$$

On the other hand, the surface area corresponding to the "spherical" pore shape assumption is described through[28]:

$$S_{0_{\text{sphe}}} = 6\cdot V_{\text{Cu}_2\text{O}}\cdot\sum_{i=1}^{N}\frac{\phi_i}{d_{\text{Cu}_2\text{O}_i}} \quad (11)$$

The actual pore wall surface area will be an intermediate value between those two:

$$S_0 = \alpha\cdot S_{0_{\text{sphe}}} + (1-\alpha)\cdot S_{0_{\text{cyl}}} \quad (12)$$

where $\alpha$ goes from zero (perfectly cylindrical pores) to 1 (pore morphology in Kiil et al.[28]).

As a means of accounting for the possible overlapping of the pores resulting from the binder loss from the pore walls, the random pore model is used.[49] Although this early model was based on the reaction of pure solids with perfectly cylindrical pores and pure kinetic control, it is still believed that it can provide a useful description of the dependency of the reaction surface with the solid conversion. The expression used is:

$$\frac{S(X_{\text{ZnR}})}{S_0} = \frac{1-\varepsilon(X_{\text{ZnR}})}{1-\varepsilon_0}\sqrt{1-\psi\cdot\ln\left(\frac{1-\varepsilon}{1-\varepsilon_0}\right)},$$

$$\psi = \frac{4\cdot\pi\cdot L_p\cdot(1-\varepsilon_0)}{S_0^2} \quad (13)$$

where $\psi$ is a parameter that depends on the initial porous structure (completely leached paint). To estimate the initial total pore length per unit volume of our system, the number of pores per surface unit is again assumed to be equal to the number of soluble pigment particles per surface unit (non-interconnected pores). There is no experimental evidence to question the use of $\psi$ values determined from purely structural considerations.[50] The value obtained for $\psi$ in this work is close to zero, which involves a continuous decrease of the exposed surface per total volume with increasing binder conversions.[51] The total change in active (that is, ZnR) pore surface area with time can subsequently be described through:

$$S_0(t)\big|_1 = S_0\cdot\left(\frac{S(X_{\text{ZnR}})}{S_0}\right)\Bigg|_1\cdot f_{\text{ZnR}}(t)\big|_1 \quad (14)$$

where $f_{\text{ZnR}}$ accounts for the varying fraction of pore walls being the resinate (see Eqs. 15 and 16 below).

*Pore Wall Composition.* The possibility of unreacted ZnR becoming exposed after the dissolution of their neighbor ZnR molecule is accounted for through:

$$f_{\text{ZnR}}(X_{\text{ZnR}})\big|_1 = \frac{V_b\cdot f_{\text{ZnR}}\cdot(1-X_{\text{ZnR}}(t)\big|_1)}{(1-V_{\text{Cu}_2\text{O}})-V_b\cdot f_{\text{ZnR}}\cdot X_{\text{ZnR}}(t)\big|_1} \quad (15)$$

The value of Eq. 15 at time t = 0 assumes that the insoluble particles can also be exposed at the pore walls.

If a soluble plasticizer is used, it is assumed that it leaches the paint together with the resin in the same ratio as they were added to prepare the paint (rough approximation[33]). Thus, in this case, Eq. 16 simplifies to:

$$f_{\text{ZnR}}(X_{\text{ZnR}})\big|_1 = \frac{V_b\cdot f_{\text{ZnR}}\cdot(1-X_{\text{ZnR}}(t)\big|_1)}{(1-V_{\text{Cu}_2\text{O}})-V_b\cdot X_{\text{ZnR}}(t)\big|_1} \quad (16)$$

While these simplistic expressions are expected to properly describe the variation in the pore wall composition during the somewhat early stages of exposure, it is most likely that they fail when the binder conversion reaches relatively high values, such as those reported in Yebra et al.[32] In those cases, it is possible that the probability of exposing a fresh ZnR molecule after the binder dissolution is incorrectly described by Eqs. 15 and 16 as a result of the high amounts of insoluble binder components that may protect isolated ZnR groups.

***Moving pigment front ($l_{s1}$)***

The equations governing the dynamics of the $Cu_2O$ dissolving front remain the same as in the TBT-SPC model. However, the concentration of the species involved in the reaction may vary from the TBT-SPC case due to, e.g., $Cu^+$ oxidation and reactions involving pH changes, such as the formation of $Zn(OH)_x^{2-x}$ species (see equations later on and Supplementary Material).

$$\frac{dl_{s1}}{dt} = \frac{M_{Cu_2O} \cdot \left( D_{e,CuCl_2^-}(t) \cdot \frac{d[CuCl_2^-]}{dl} + D_{e,CuCl_3^{2-}}(t) \cdot \frac{d[CuCl_3^{2-}]}{dl} + D_{e,Cu^{2+}}(t) \cdot \frac{d[Cu^{2+}]}{dl} \right)\Big|_{1=1_{s1}}}{2 \cdot (1-\varepsilon_o) \cdot V_{Cu_2O} \cdot \rho_{Cu_2O} \cdot (1-V_I)} \tag{17}$$

with the initial condition

$$1_{s1}(t=0) = 0 \tag{18}$$

In the balances performed to the leached layer (see Supplementary Material), a symmetric (no penetration) boundary condition is placed at the dissolving pigment front.

$$\left( D_{e,CuCl_2^-} \frac{d^2[CuCl_2^-]}{dl^2} + D_{e,CuCl_3^{2-}} \frac{d^2[CuCl_3^{2-}]}{dl^2} + D_{e,Cu^{2+}} \frac{d^2[Cu^{2+}]}{dl^2} \right)\Big|_1 = 0 \tag{19}$$

The boundary condition at $l_{s1}$:

(1) If water penetration beyond the pigment front is a possibility:

$$([CuCl_2^-] + [CuCl_3^{2-}])|_{1_{s1}} = f_{sat} \cdot [Cu(I)]_{sat} \tag{20}$$

The parameter $f_{sat}$ depends on the degree of protection of the pigment particles by the binder. If the resin is so hydrophilic that a large $Cu_2O$ particle surface is exposed to seawater, the $f_{sat}$ factor approaches unity (see discussion later on).

(2) Otherwise, if the kinetic expression determined by Ferry and Carritt applies[28,36]:

$$\left( D_{e,CuCl_2^-} \cdot \frac{d[CuCl_2^-]}{dl} + D_{e,CuCl_3^{2-}} \cdot \frac{d[CuCl_3^{2-}]}{dl} \right)\Big|_{1_{s1}} = 2 \cdot (-r_{Cu_2O})|_{1_{s1}} \cdot f_{Cu_2O} \tag{21}$$

for the calculation of the reverse reaction constant[28]:

$$k_{-1} = 2 \cdot k_1 \cdot \frac{K_w \cdot a_w}{K_{CuCl_2^-} \cdot L_{CuOH} \cdot \frac{\gamma_{Cl^-} \cdot \gamma_{H^+}}{\gamma_{CuCl_2^-}}} \tag{22}$$

***Moving paint surface ($l_{s2}$ or polishing front)***

In the TBT-SPC model, no paint polishing was assumed to occur until the $X_{max}$ conversion value was attained at the paint surface. The reason was that the binder can be assumed sufficiently strong to withstand the shear forces exerted by the moving seawater for low values of binder conversion ($<X_{max}$). The $X_{max}$ value varied with the sailing speed of the vessel, thus stressing the combined role of chemistry and erosion on the polishing of TBT-SPC. In paints with high rosin content, the role of erosion in the polishing process is even more marked than in the TBT-SPC case. Hence, in contrast to an on/off approach to the erosion process, it seems more realistic to assume that the surface polishing commences as soon as the vessel starts moving, without any significant paint degradation. At short exposure times, the erosion rate (g binder·cm$^{-2}$·day$^{-1}$) of virtually unreacted paint binders is markedly slower than the binder degradation rate (g ZnR·cm$^{-2}$·day$^{-1}$), so that the chemical conversion at the surface increases with time. However, and as a result of the latter weakening process at the paint surface, the erosion rate increases progressively until a constant value is reached. At that point of binder conversion (i.e., $X_{max}$), the amount of binder that reaches $X_{max}$ per unit time is equal to the erosion rate so that a pseudo steady-state is attained. Such a value is calculated in a similar way as in the TBT-SPC model. Thus, in the current model, the following mathematical expression was initially used to model the polishing process:

$$\left(\frac{dl_{s2}}{dt}\right)_{X_{ZnR}|_{1_{s2}}} = \left(\frac{dl_{s2}}{dt}\right)_{X_{max}} \cdot \frac{X_{ZnR}|_{1_{s2}}}{X_{max}} \text{ for } t \le 0 \le t_{max} \tag{23}$$

where $t_{max}$ is the value of time corresponding to the surface conversion, $X_{ZnR}|_{1_{s2}}$, being equal to $X_{max}$ (could be estimated by monitoring the surface conversion as a function of exposure time[32]).

Once the binder conversion at the paint surface has reached the $X_{max}$ value, the paint attains a stable polishing rate, which can be represented by[28]:

$$\frac{dl_{s2}}{dt} = \frac{-\left(\frac{\partial X_{ZnR}}{\partial t}\right)\Big|_{1=1_{s2}}}{\left(\left(\frac{\partial X_{ZnR}}{\partial l}\right)\Big|_{1=1_{s2}}\right)_t} \text{ for } t > t_{max} \tag{24}$$

with

$$1_{s2}(t=0) = 0 \tag{25}$$

as the initial condition.

Equation 24 summarizes the strong point of the $X_{max}$ theory: one can a priori model erosion rates by looking at the dynamics

of the binder conversion. In other words, if a complete quantitative description of the binder reaction rate is available, knowledge of the pseudo-steady state binder conversion profile along the leached layer can be used to calculate the rate at which the paint surface is being removed by seawater friction forces. Actually, the latter holds even if the reaction we model is not directly involved in the polishing process.

### *Local conversion*

The local conversion of the ZnR in the leached layer is given by a mass balance:

$$\left.\frac{\partial X_{\mathrm{ZnR}}}{\partial t}\right|_1 = \frac{S_0(X_{\mathrm{ZnR}})|_1 \cdot (-r_{\mathrm{ZnR}})|_1 \cdot M_{\mathrm{ZnR}}}{(1-\varepsilon_0)\cdot(V_b \cdot f_{\mathrm{ZnR}}(t=0))\cdot \rho_{\mathrm{ZnR}}} \tag{26}$$

with the initial condition

$$X_{\mathrm{ZnR}}(1, t=0) = 0 \tag{27}$$

### *Chemical speciation*

During immersion, the activity of the AF paint results in the release of $Zn^{2+}$ and $Cu^{+}$ species. Thus, in addition to the seawater species (i.e., $Na^{+}$, $Cl^{-}$, $H^{+}$, $OH^{-}$, $CO_2$(aq), $HCO_3^{-}$, $CO_3^{2-}$, $Mg^{2+}$, $SO_4^{2-}$, $O_2$), the distribution within the active paint zone of the following species must be determined: NaR, $Zn^{2+}$, $Zn(OH)^{+}$, $Zn(OH)_2$(aq), $Zn(OH)_3^{-}$, $ZnCl^{+}$, $ZnCl_2$(aq), $ZnCl_3^{-}$, $ZnCl_4^{2-}$, $CuCl_2^{-}$, $CuCl_3^{2-}$, $Cu^{2+}$. The equations used in the chemical equilibrium calculations can be obtained in the Supplementary Material to this article or in Yebra.[48]

### *Model parameters*

In addition to the parameters listed by Kiil et al.,[28] the new processes accounted for in the tin-free model require extra physical and chemical constants. All such parameters can be consulted in the Supplementary Material and in Yebra.[48]

### *Numerical solution technique*

The model is first rendered dimensionless by introduction of suitable dimensionless variables.[48] The moving paint and pigment fronts were tracked by means of an appropriate coordinate transformation.[28] Immobilizing and normalizing the boundaries of the thin active region (i.e., the leached layer) allows the implementation of an orthogonal collocation numerical solution procedure[52] in which four interior collocation points are sufficient to attain convergence, despite the steep concentration gradients developed.

## Results and Discussion

### *Uncertain model parameters*

In the mathematical AF paint description presented above, four parameters deserve a more thorough discussion prior to analyzing the model performance. These are the tortuosity factor ($\tau$), the exposed pore surface area ($S_0$), $f_{sat}$, and $X_{max}$. For TBT-SPC model paints, Kiil et al.[28] estimated the tortuosity factor of the leached layer from the PVC and PSD of $Cu_2O$ particles, according to an expression derived for pellets of compressed catalyst particles (i.e., different pore origin[47]). Although such an assumption was fairly successful when applied to TBT-SPC model paints, it leads to simulations that largely underestimate the leaching rates observed experimentally in rosin-based model paints.[32] Presumably, the latter is due to the different mechanical properties of the paint systems (see model assumptions above). In this work, for paints in which leached layers were clearly visible, the tortuosity factor value is estimated by independently modeling the experimental leaching rates after assuming saturation of Cu(I) species at the pigment front (unless large amounts of hydrophobic co-binders are added; see discussion below). In order to do that, the polishing rate was first fixed externally so as to follow the experimental trend, and the tortuosity factor was subsequently adjusted to match the experimental behavior. The fact that all the other leaching parameters (e.g., diffusion coefficients) are well characterized means that a representative value for the tortuosity factor can be attained.

Once the tortuosity factor is determined, the next step is to determine the pore wall surface area ($S_0$) that properly describes the polishing data acquired through the rotary tests. In good agreement with the low tortuosity values (in the range from 1.3 to 2.5) determined from the leaching modeling, the pore structure developed in tin-free paints is hypothesized to be significantly broader than in TBT-SPC paints, somewhere in between the tortuous cylindrical pore morphology detailed in the model development section (see Eq. 10) and that assumed in the TBT-SPC model (see Eq. 11). The actual pore surface, in relation to such idealistic geometries, is given by the parameter $\alpha$ (see Eq. 12).

The use of a rosin derivative plasticized by a hydrophilic resin is expected to allow water penetration beyond the pigment front. Thus, $Cu_2O$ particles away from that position will also be subjected to chemical attack and will generate soluble chloro-complexes. Unlike the complexes generated at the pigment front, the dissolved Cu(I) species formed beyond the pigment front will encounter a very difficult diffusion path until they reach the open pores of the leached layer. Consequently, high concentrations (that is, saturation) of these complexes are expected to develop up to the leaching front. Accordingly, the shorter the distance that water can penetrate into the unreacted paint film, the lower the concentration level of Cu-complexes at the leaching front. Hence, when large amounts of hydrophobic resins are used (that is, Ti-5), an extra parameter, termed $f_{sat}$, accounting for the ratio between the concentration of Cu-complexes at $l_{s1}$ and that of saturation at the local pH and $Cl^{-}$ concentration is introduced in order to match the experimental results. Another potential interpretation of $f_{sat}$ is related to the Marson's osmotic breakdown process. While in the TBT-SPC model[28] that process was found not to influence the copper leaching kinetics, it is possible that when lower amounts of soluble pigments are used together with very hydrophobic resins and insoluble pigment particles (that is, longer distance between particles), there exists a time delay related to the water permeation process through the binder membrane, which slows down the leaching process.

Finally, an estimation of the $X_{max}$ parameter was provided through SEM-EDX measurements in Yebra et al.[32] using the method proposed in the TBT-SPC model.[28] Despite the uncertainties discussed in Yebra et al.,[32] it seems that binder conversion values of around 0.5-0.7 are attained at the paint surface after just a few weeks of immersion.

### *Performance of paints containing* $Cu_2O$ *and insoluble pigment particles*

Insoluble pigment particles are used in antifouling paint products not only because of their evident aesthetic function (these pigments remain in the leached layer and determine the paint color in service), but also because they can be used to tailor-make the paint performance (such as they influence the mechanical resistance and the morphology of the leached layer). Therefore, a mathematical description that accounts for the effects of these ingredients on the paint activity would constitute a very interesting step forward towards the understanding of AF paint systems (it was not included in the TBT-SPC model). Additionally, the fact that leached layers are easily formed when these pigments are used (that is, $X_{max}$ can be estimated[32]) will allow us to test whether the mathematical model presented above has indeed captured the main paint activity mechanisms properly.

Details about the modeling of paints containing high loads of seawater soluble $Cu_2O$ pigments and no insoluble particles can be found in Yebra.[48] The absence of leached layers in most of these paints makes the model-based analysis rather speculative, though in agreement with those to be presented below.

If the polishing behavior of the paints described in Table 1 is modeled based on the same principles as the TBT-SPC model[28] (with the amendments presented in this article), a very good match between experimental performance data and model predictions is attained for most $TiO_2/Fe_2O_3$-containing paints[48] if cylindrical pores are assumed (that is, $\alpha = 0$, see Eq. 12) with low tortuosity factor values and the $X_{max}$ binder conversion values measured.[32]

Nevertheless, for paints Ti-1 and Fe-1, the model predicts that the $X_{max}$ conversion values[32] are reached at the paint surface after almost two months of immersion. Experimental evidence pointing at a fast attainment of the $X_{max}$ surface conversion values have been presented.[32] This mismatch is even more obvious in paints Ti-2 and Ti-3. In those paints, which contain larger $Cu_2O$ and $TiO_2$ amounts, the $X_{max}$ values that match the experimental data are about 30% higher than those measured by SEM-EDX.[32] Furthermore, these surface conversion values are only reached after more than three months of immersion, contradicting the evidence presented in Yebra et al.[32]

*Discussion on the Polishing Assumptions.* The experimental AF model paint performance presented elsewhere[32] for $TiO_2$ containing paints cannot be modeled through the traditionally assumed polishing mechanism under the assumptions made in this work. According to the model if, for example, paint Ti-3 reacts fast enough so as to reach the $X_{max}$ binder conversion within 2-3 weeks of exposure,[32] the surface conversion should continue increasing given the low polishing rate observed experimentally. In other words, the amount of binder removed by erosion per unit of time is less than that predicted to react over the $X_{max}$ value. It thus seems that the binder reaction is markedly slowed down at a conversion value of about 0.5-0.7 (see Figure 3). The latter would also explain the flat binder conversion profile measured along the leached layer of paint Ti-3.[32]

Let us assume that a pre-leached (that is, $Cu_2O$-depleted) paint is exposed to seawater. Will the binder conversion value ever reach unity? Is some binder "sheltered" by insoluble paint components so that it is unavailable for reaction with seawater? Is the pore wall surface blocked somehow, hindering the reaction of the underlying ZnR molecules? An interesting result is that obtained for paint Ti-5 in Yebra et al.[32] This paint showed no significant polishing, which means that the paint surface was exposed to seawater for the entire testing time (that is, 14 weeks). The EDX profile of this paint shows a surface conversion value of about 0.65, that is, a similar value to that measured for paint Ti-2, which incorporates the same pigment load. The low copper leaching rate observed in this paint seems to discard a significant role of copper (that is, formation of copper resinates[33]) on the blocking process. Also, samples exposed to 0.025 M sodium glycinate buffer ($NH_2$-$CH_2$-COONa; 32 g/l NaCl; fast leaching of both soluble binder and $Cu_2O$) seemed to confirm the hypothesis of a maximum binder conversion value.[32]

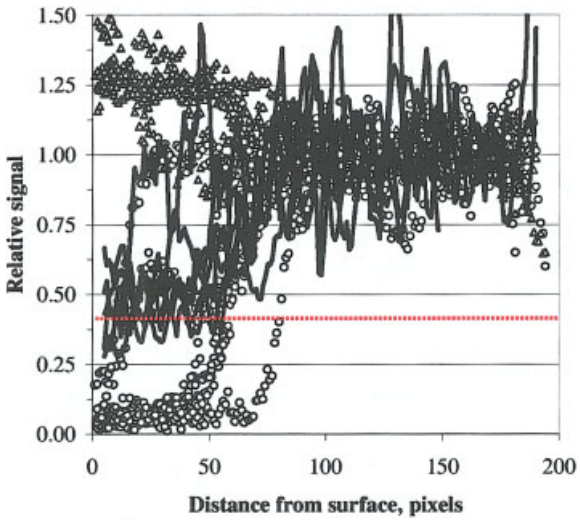


**Figure 3. Zn profiles along the leached layer corresponding to several samples of paints Ti-1, Ti-2, Ti-3, and Ti-5 exposed to seawater for different times in the rotary setup.[32]**

Triangles correspond to Ti signals and circles to Cu signals. The lines correspond to trend lines (moving-average) showing the Zn profile. An indication of the size of the leached layer thickness corresponding to the different paints can be obtained by looking at the Cu profiles. [Color figure can be viewed in the online issue, which is available at www.interscience.wiley.com.]

*Preliminary Simulations with a Maximum Binder Conversion Value.* The hypothesis of a maximum binder conversion was further tested by means of the model. The experimental polishing rate measured for paint Ti-3 was imposed to the model. At the same time, and independently, the pore walls were allowed to react assuming different pore geometries. Whenever a binder conversion value equal to the $X_{max}$ ones measured in Yebra et al.[32] was reached anywhere within the leached layer, the binder was not allowed to react any further. The results of the simulations are shown in Figures 4 and 5. Some conclusions can be extracted from those plots:

- The use of relatively low surface area pores, that is, $\alpha$ values about 0.5, seems to reproduce the EDX profiles best (Figure 4), although the experimental results might be too uncertain to confirm this. It must be stressed that the results in

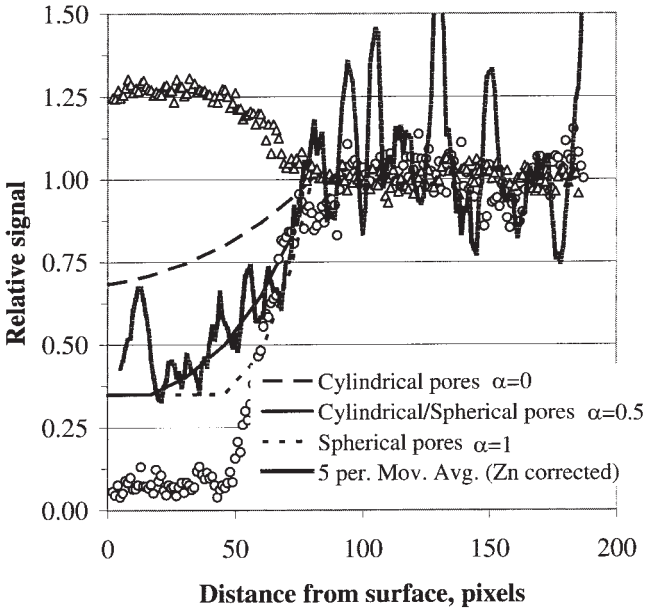


**Figure 4. Predicted ZnR conversion profile along the leached layer for paint Ti-3 after three weeks of immersion.**

Three different pore geometries were used in the first plot: cylindrical pores, "spherical" pores,[28] and an intermediate surface area between those two.

Figure 4 were attained by assuming the surface renewal rate given in Eq. 16. In agreement with the maximum conversion hypothesis, we might expect that the binder reaction becomes progressively slower as a result of the increasing proportion of insoluble binder ingredients. If that is the case, larger pore wall surface area values will be needed to match the experimental data.

- A constant polishing rate from time t = 0 seems to properly describe the polishing behavior of paint Ti-3. Actually, going back to Yebra et al.,[32] we can realize that a constant polishing rate would fit all the experimental results fairly well (Figure 5). Such an assumption implies that the loss of, e.g., 60% of the initial ZnR (that is, about 50% of the binder phase volume) does not lead to any significant difference in the erosion resistance of the paint surface. The latter does not seem very realistic, so it is most likely that the assumption of increasing polishing rates with higher binder conversion values still holds (see Eq. 23), although the time to reach a stable surface conversion value is significantly shorter than that predicted by the full model (higher $\alpha$ values and, subsequently, binder reaction rates apply).
- The tortuosity factor values used in the full model, together with the assumption of Cu(I) saturation at the pigment surface, are still the only way of matching the experimental leaching results under the model assumptions listed at the beginning of the article (see Figure 5).

*Proposed Working Mechanisms for Rosin-Based Antifouling Paints.* Based on the evidence discussed above, a first proposal for the working mechanisms of the relevant rosin-based paints can be performed. $Cu_2O$ leaches fairly fast due to a relatively easy water penetration through the paint film. If the paint surface contains significant amounts of insoluble pigments or resins, the initial erosion rate will be slower than the leaching rate (slower the higher the insoluble pigment/resin content[48]) so a leached layer will be formed. The pores of such a leached layer are characterized by a fairly open structure of low tortuosity. The latter is attributed to the fact that the walls delimiting the pores are relatively thin and brittle. Hence, they are believed to collapse easily as a result of the osmotic stresses built up due to the presence of soluble components in the paint film. The higher the amount of soluble pigment particles (that is, the shorter the interparticle distance and the thinner the leached layer walls), the more likely it is that the walls collapse partially, leading to more open pores (that is, less tortuosity). When comparing paints Ti-1, Ti-2, and Ti-3, the PVC of $Cu_2O$ (that is, soluble pigments) seems to influence the pore tortuosity much more than that of $TiO_2$ (that is, insoluble pigments).

The rough walls and the very fast leaching of soluble plasticizer resins should lead to a fairly high ZnR exposed surface area and a subsequently fast depletion of the controlled release resin. However, after just a few weeks of immersion, the ZnR reaction is markedly slowed down and it is the erosion of the insoluble paint components and about 35% of the initial ZnR that determine the polishing rate of the paint. According to the rotary data, the fact that the surface of paint Ti-3 is more porous that that of paint Ti-2 (i.e., larger $Cu_2O$ content) poses no visible effects on the polishing rate, probably because Ti-3 appears to have slightly higher residual ZnR amounts at the surface than paint Ti-2.[32]

In the light of Figure 4, it seems unlikely that paint Cu-3 develops pores that are well described by the cylindrical pore assumption, unless a significant pore collapse takes place as a result of the large $Cu_2O$ amounts. Analogously to the $TiO_2$-containing paints, it seems reasonable to speculate that these paints also reach a conversion value in which the insoluble paint components virtually stop the ZnR dissolution process. Nevertheless, this conversion value will probably be higher than in the $TiO_2$-containing paints due to the larger binder surface area exposed.

*Effect of Strongly Hydrophobic Resins on the Cu-Leaching Rate.* The effects of the co-binder resin properties on the leaching rate are further investigated in Figure 6, where two different formulations incorporating dissimilar binder systems but the same pigment load are compared. As already mentioned, the leaching rate observed for paints containing the base case binder[32] is very high. Cu(I) saturation at the pigment front and a low resistance to diffusion through the leached layers must be assumed in order to match the experimental trends. If, e.g., paint Ti-2 was assumed not to polish, leached layers of up to 80 $\mu$m would develop in just a few weeks of seawater immersion (see Figure 6). On the other hand, the addition of large amounts of a hydrophobic resin leads to a very low leaching rate (Figure 6). There are two potential mechanisms through which this co-binder can slow down the leaching process:

- By diminishing the soluble pigment area exposed. The latter might lead to lower Cu(I) accumulation at the pigment front or, if only the uppermost pigment surface is exposed, to mixed kinetic/diffusive control of the dissolution rate.[28]
- By limiting the water permeation through the interparticle binder membrane. In hydrophobic binders, the step from one pigment particle to another, neglected in the model up to now, might need to be considered.

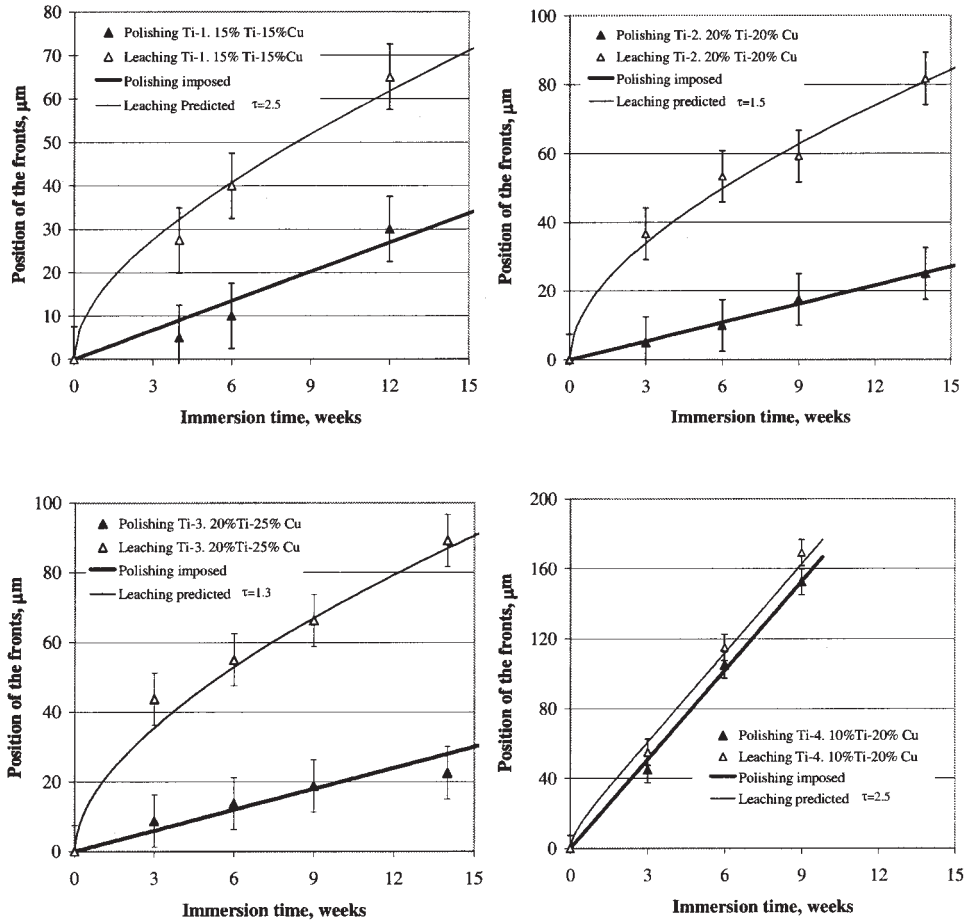


**Figure 5. Experimental (symbols) and predicted (lines) position of the polishing and leaching front for different Ti-containing paints.**

The polishing rate was imposed to a constant value. The surface conversion was allowed to reach a maximum value (see Yebra et al.[32] for $X_{max}$ and paint compositions).

The assessment of the first possibility leads to relatively low but somewhat steady leaching rates (Figure 6) and, subsequently, increasing leached layer thicknesses. In such a figure, a stabilization of the leached layer thickness measured can be observed despite the absence of paint polishing. Thus, the second assumption seems more appropriate. It is also likely that, in that case, the presence of $TiO_2$ particles leads to the formation of "dead-ends" in the pore network, that is, the insoluble pigments and the hydrophobic binder prevent the water molecules from reaching the next $Cu_2O$ particle. If the paint does not polish (such as Ti-5), the number of such "dead-ends" would increase with immersion time, eventually blocking the leaching completely. Accordingly, the copper leaching process would commence fairly fast, rapidly slowing down to a fairly low leaching rate.

Something similar applies to strongly hydrophobic inert acrylic paints formulated with $40\%_{sv}$ $Cu_2O$ and tested in the rotary set-up. Only 5-10 $\mu$m of leached layer (that is, the first one or two $Cu_2O$ layers) were observed after the first inspection and, from that point on, the paint remained unaltered all through the testing period (results not shown). Only the blocking of the permeation/osmotic breakdown process described by Marson[37] can explain such behavior.

As no mathematical expression accounting for the latter process is incorporated into the paint model, only a very low relative Cu(I) saturation at the pigment front must be used if a tortuosity factor value in the same range as the other paints tested is to be used (Figure 6). A different combination of $f_{sat}$ and tortuosity factor would have led to very similar results, so the true leaching mechanisms of paint Ti-5 are still unresolved.

We hypothesize that the control of the water permeation beyond the pigment front by the use of a proper load of insoluble pigments and hydrophobic resins (which, at the same time, does not impede a suitable polishing rate) is the key to the success of a $Cu_2O$-based AF formulation.

### *Improved knowledge of this model paint system*

The analysis performed above demonstrates the advantages of this new analysis tool for the design and optimization of AF paints. While only leaching and polishing rates would have been obtained from a simplistic evaluation of the rotary tests, indications about, e.g., the pore morphology and the detailed leaching and polishing mechanisms can be attained by use of the model (see Table 2). Even if only few definite conclusions about how these paints work are presented in this article, the

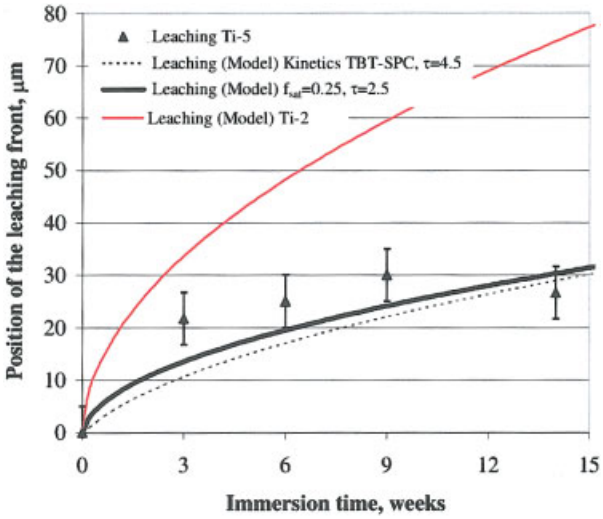


**Figure 6. Experimental (symbols) and simulated (lines) position of the leaching front for paints containing 20%$_{sv}$ $Cu_2O$ pigments and 20%sv $TiO_2$ (25°C, pH 8.2[32]).**

To describe the leaching of paint Ti-5 (symbols), a different leaching mechanism compared to paint Ti-2 (red line; no polishing assumed) must be considered. Modeling-wise, lower Cu(I) concentrations at the pigment front and higher tortuosity values have to be used (solid line). The use of similar copper leaching assumptions as in the TBT-SPC paint model also yields satisfactory results (dashed line). We conclude that the high hydrophobicity of Hydrophobic resin 3 effectively limits the penetration of water beyond the dissolving $Cu_2O$ front. [Color figure can be viewed in the online issue, which is available at www.interscience.wiley.com.]

intention is to show how a detailed analysis of the paint behavior raises some fundamental questions about the paint activity mechanisms, the answers to which might provide crucial hints for the identification of a successful and clean AF technology.

The mathematical model presented in this article allows the estimation of the pH within the leached layer as a function of the leaching rate (which consumes $H^+$ ions), carbonate buffer concentration (that is, seawater composition), and so on. The latter is important to understand the behavior of controlled release binders within paint systems, especially for pH sensitive binders, such as the rosin derivative used in this study.[33] Also, "hidden" variables such as the $Cu^{2+}$ concentration within the leached layer can be investigated. In Figure 7, a picture of paint Ti-3 after 14 weeks of exposure is shown. When looking closely at the leached layer in the proximities of the leaching front, it is indeed possible to appreciate a greenish color, which is traditionally associated with inorganic basic copper carbonates (BCCs).

The formation of chloro-copper complexes in seawater is thought to stabilize the $Cu^{2+}$ ions in solution and "protect" them from reacting with $OH^-$ and $CO_3^{2-}$ anions forming insoluble compounds.[1] If the value suggested for the BCC solubility in seawater in WHOI[1] is used, Figure 7 shows that no precipitation is predicted within the leached layer. Contrarily, when the S-L equilibrium $Cu(OH)_2$ is considered, $Cu^{2+}$ concentration values close to saturation are predicted. If even more insoluble salts, such as malachite ($Cu_2(OH)_2CO_3$), azurite ($Cu_3(OH)_2(CO_3)_3$), or, generically, $Cu_x(OH)_y(CO_3)_zCl_{2x-y-2z}$,[1,53,54] are taken into account, then the formation of inorganic $Cu^{2+}$ precipitates is found to be thermodynamically stable in the proximity of the pigment front. A thorough analysis of the effect of copper leaching rates, leached layer thickness, leached layer tortuosity factor, and seawater conditions (that is, pH, temperature, salinity, dissolved $O_2$) on the possibility of BCC precipitation can be easily performed with the model.

Once a complete description of the leaching process is attained (that is, dissolution rate and leached layer morphology as a function of paint parameters), it is straightforward to obtain copper leaching rate predictions during, for example, the first month of immersion, if the polishing rate can be neglected

**Table 2. Model Key Parameters and Their Significance**

| Key Parameters | Description | Value | Conclusions |
|---|---|---|---|
| $f_{sat}$ | Ratio of the concentration of chloro-copper complexes at the pigment front relative to the saturation value | Fitted through the independent modeling of the leaching process (imposing the polishing rate). It is equal to 1 for paints with a large rosin content and low hydrophobic co-binder content. | In rosin-based model, saturation of copper-complexes at the pigment front seems to apply. Copper leaching is thus purely diffusion-controlled. $f_{sat}$ can be used to account for different degrees of hydrophobicity resulting from the use of larger amounts of inert co-binders or improved ones. |
| $\tau$ | Tortuosity factor | Fitted through the independent modeling of the leaching process (imposing the polishing rate). Low values, ranging from 1.3 to 2.5, were used in this study. | Adjustable parameter used to characterize the tortuosity of the leached layer pores. It seems that in paints with a large rosin content, the pore structure is more open compared to TBT-SPCs, probably due to poorer mechanical properties and a larger content of leaching binder components. |
| $\alpha$ | Pore morphology parameter | Fitted through the independent modeling of the binder reaction. The polishing rate is imposed and the $Cu_2O$ leaching is modeled after fitting $f_{sat}$ and $\tau$. A value of 0.5 seems realistic. | Adjustable parameter used to characterize the pore surface area of the leached layer. It seems that in paints with a large rosin content, the pore structure is more open compared to TBT-SPCs. |
| $X_{max}$ | Value of surface conversion of the active binder when the paint reaches a stable polishing rate | Measured through SEM-EDAX. 0.5–0.75. See Yebra et al.[32] for details. | In paints with a large rosin content, a maximum binder conversion is attained fast all through the leached layer, and it is the surface erosion of such chemically-weakened surface that determines the polishing rate. |

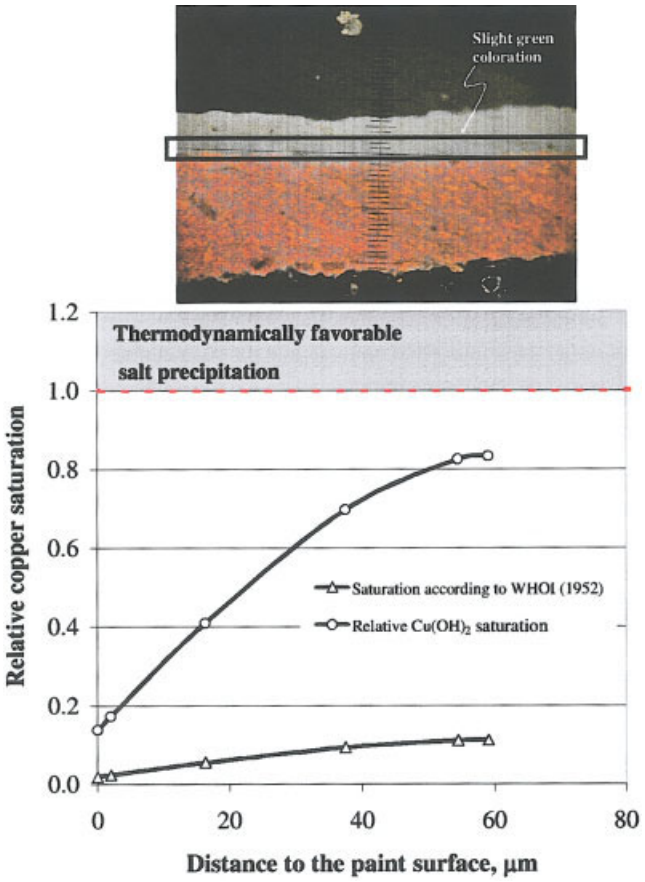


**Figure 7. Picture of paint Ti-3 in which a greenish coloration can be seen close to the pigment front (top); such a scenario can be predicted by using thermodynamic data of inorganic copper compounds.**

In the bottom plot, the relative saturation values predicted by the model along the leached layer of paint Ti-3 are shown. Two different approaches are used for the BCC saturation point. [Color figure can be viewed in the online issue, which is available at www.interscience.wiley.com.]

(for example, commercial paints at mild shear stress conditions, such as those employed in the ASTM D6442–99 method[55]) or estimated (Figure 8). Optimally, such information could be acquired for a large number of paints through simple, accelerated, laboratory experiments. Thus, within a few days, many formulations could be pre-tested with the model as regards the copper leaching rate (for example, one day of experiment plus one minute of simulation replacing several weeks of test). The model also allows a detailed comparison of the leaching mechanisms depending on the formulation by, for example, externally equalizing the polishing rates of two different paints (for example, Ti-2 and Ti-5) to subsequently compare their respective leaching behavior directly (see Figure 8). That could also have been done to compare the leaching mechanism of the TBT-SPC model paints tested in Kiil et al.[28] and a similar rosin-based paint tested in this work. Thus, the model can yield detailed knowledge about the differences in the activity mechanisms of markedly different AF paint systems.

## Conclusion

Statistical experimental design is certainly the best way of identifying the optimal combination of a given set of raw materials as regards the AF paint performance. However, such an empirical approach leaves too many unanswered questions, which become serious obstacles in the search for new raw materials or ideas improving the AF paint performance. The latter is also true for those technologies that try to incorporate more environmentally benign compounds while keeping the excellent performance associated with technologies based on the release of slowly-degrading biocides into the marine environment. We believe that a thorough knowledge of the underlying activity mechanisms of AF paint will help in providing detailed information on the paint behavior, which will lead to innocuous and effective AF products.

In this context, a generic mathematical model for chemically-active antifouling paints has been developed and tested for rosin-based $Cu_2O$-containing model paints. This model re-

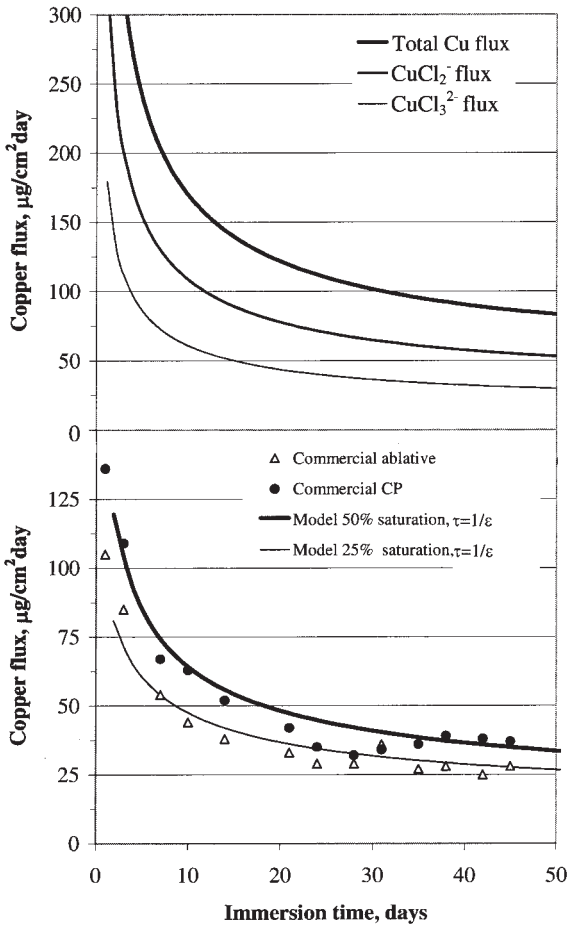


**Figure 8. Predicted copper leaching rate predicted for paint Ti-3 (top).**

The good match between the model output and the experimental data implies that a very accurate representation of the evolution of the leaching rate with immersion time has been attained for that paint. In the bottom plot, the experimental ASTM D6442–99 data obtained by Haslbeck and Holm[55] are plotted against the model predictions. A polishing rate of 5 $\mu$m/month is assumed, with 20%$_{sv}$ $Cu_2O$ as the only soluble pigment. The simulated seawater conditions and the rotor dimensions and speed are those specified in the standard.

quires quantitative knowledge of the seawater reaction rate of the controlled-release resin and of the pore morphology (mainly dependent on the pigment load and binder characteristics), an understanding of the polishing mechanism, and a description of the dissolution rate of the soluble pigments. The new model also contains a more detailed modeling of the seawater speciation by use of the Extended UNIQUAC ion activity coefficient model.[56] Also, the Cu(I) oxidation process is also included for the first time. Compared to AF products based on tin-containing acrylic polymers, paints with a large content of rosin derivatives have shown a faster biocide leaching rate as a result of enhanced water ingress into the paint film and a relatively open leached layer structure. The polishing rate is shown to depend on the erosion of the paint surface, which has been weakened by seawater reaction of the rosin-based binder components.

The capabilities of mathematical modeling for the study of chemically active antifouling paints have already been detailed elsewhere.[22,28-31] However, and compared to the TBT-SPC modeling work, this study has demonstrated that:

- It is not possible to predict the seawater behavior of any chemically active antifouling systems based on a priori mechanistic assumptions (such as the $Cu_2O$ dissolution kinetics successfully used by Kiil et al. may not be valid elsewhere due to different binder hydrophilicity).
- Related to that, mathematical modeling, helped by a number of experimental tests,[32,33] is a unique tool to elucidate the working mechanisms of chemically-active antifouling paints.
- The analysis of the results suggests simple tests for the screening of new paint ingredients at the same time that they set quantitative specifications for the optimizing ingredients.

## Acknowledgments

The work presented in this article was financially supported by The Danish Technical Research Council. Associate Professor Kaj Thomsen (IVC-SEP) and Dr. Jorge Marrero Morejón (CAPEC), also from the Department of Chemical Engineering of DTU, helped with the estimation of some model parameters.

## Notation

$a_i$ = activity of species i, mol/m$^3$
$d_{Cu_2O_i}$ = $Cu_2O$ particle diameter corresponding to the volume fraction $\phi_i$, m
$\bar{d}_{Cu_2O}$ = mean diameter of the $Cu_2O$ particles, m
$D_{e,i}$ = effective diffusivity of component $i$ in the leached layer, m$^2$s
$f_{ZnR}$ = initial binder volume fraction being ZnR, m$^3$ZnR/m$^3$ binder
$f_{sat}$ = ratio of the concentration of chloro-copper complexes at the pigment front relative to the saturation value
$f_{Cu_2O}$ = surface fraction occupied by $Cu_2O$ particles, $m^2_{Cu_2}O/m^2_{Paint}$
$[i]$ = concentration of species $i$, mol/m$^3$
$k_1$ = kinetic constant for the seawater reaction of ZnR, [(mol $Zn^{2+}$)/(m$^2$ film) · s] · (m$^3$/mol)$^a$
$k_{-1}$ = kinetic constant for the reverse seawater reaction of ZnR, [(mol $Zn^{2+}$)/(m$^2$ film) · s] · (m$^3$/mol)$^{b+c}$
$K_i$ = chemical equilibrium constant for reaction $i$, different units
$l$ = position in the paint film, m
$L_p$ = initial dry film thickness, m
$L_i$ = solubility constant, diverse units
$M_i$ = molar mass of species $i$, g/mol
$N_{pores}$ = number of pores formed from the dissolution of $Cu_2O$ particles
$r_{Cu_2O_i}$ = $Cu_2O$ particle radius corresponding to the volume fraction $\phi_i$, m
$\bar{r}_{Cu_2O}$ = mean radius of the $Cu_2O$ particles, m
$r_i$ = rate of reaction for the system $i$, different units
$S_0$ = initial specific surface area of exposed binder in the leached layer, m$^2$/m$^3$
$\bar{S}_{Cu_2O}$ = mean exposed area of a spherical $Cu_2O$ particle, m$^2$
$S_{pores}$ = total pore surface area per unit paint surface assuming a completely leached paint, $m^2_{pore}/m^2_{paint}$
$t$ = time, s
$t_{max}$ = time to reach the $X_{max}$ binder conversion value at the paint surface, s
$V_i$ = volume fraction of species $i$
$X$ = conversion degree
$X_{max}$ = value of surface conversion of the active binder when the paint reaches a stable polishing rate

### Greek letters

$\alpha$ = pore morphology parameter
$\gamma$ = activity coefficient
$\varepsilon$ = porosity
$\phi_i$ = volume fraction of particle size $i$
$\eta$ = viscosity, cp
$\rho$ = density
$\tau$ = tortuosity factor
$\psi$ = pore structure parameter of the Random Pore Model[49]

### Subindexes

*0* = initial (i.e., at t = 0)
*b* = binder system
*B* = value in the bulk seawater
*i* = component or species $i$
*I* = impurities
*l* = position with respect to that of the initial paint surface before immersion
*cyl* = relative to "cylindrical" pore shape
*sat* = saturation concentration
*s1* = pigment front
*s2* = film surface
*sphe* = relative to "spherical" pore shape[28]
*sv* = solids volume (i.e., calculated over the dry paint film)
*w* = water

### Abbreviations

*AF* = antifouling
*PSD* = particle size distribution
*PVC* = particle volume concentration, $\%_{sv}$ (% solids volume)
*TBT* = tributyltin
*TBT-SPC* = tributyltin self-polishing copolymer
*ZnR* = zinc resinate.

## Literature Cited

1. Woods Hole Oceanographic Institution (WHOI). *Marine Fouling and Its Prevention*. Annapolis: U.S. Naval Institute; 1952.
2. Callow ME. Ship fouling: problems and solutions. *Chemistry & Industry.* 1990;5:123-127.
3. Bertram V. *Past, Present and Prospects of Antifouling Methods*. 32nd WEGEMT Summer School on Marine Coatings, Plymouth, 2000;85-98.
4. Yebra DM, Kiil S, Dam-Johansen K. Antifouling technology: past, present and future steps towards efficient and environmentally friendly antifouling coatings. *Progress in Organic Coatings.* 2004;50:75-104.
5. Anderson CD, Hunter JE. Whither antifoulings after TBT? *NAV2000 Conference Proceedings;* 2000.
6. Rouhi AM. The squeeze on tributyltins. *Chemical and Engineering News.* 1998;76:41-42.
7. Abbott A, Abel PD, Arnold DW, Milne A. Cost-benefit analysis of the use of TBT: the case for a treatment approach. *The Science of the Total Environment.* 2000;258:5-19.
8. Townsin RL, Byrne D, Milne A, Svensen T. *Speed, Power and Roughness: The Economics of Outer Bottom Maintenance*. The Royal Institution of Naval Architects; 1980.
9. Townsin RL. The ship hull penalty. *Trans. RINA.* 1980;122:459-483.

10. Weinell CE, Olsen KN, Christoffersen MW, Kiil S. Experimental study of drag resistance using a laboratory scale rotary set-up. *Biofouling*. 2003;19 (Supplement):45-51.
11. Gerigk U, Schneider U, Stewen U. The present status of TBT copolymer antifouling paints versus TBT-free technology. *Prepr Ext Abstr ACS Natl Meet.* 1998;38:91-99.
12. Champ MA. The status of the treaty to ban TBT in marine antifouling paints and alternatives. In: *Proceedings of the 24th UJNR (US/Japan) Marine Facilities Panel Meeting in Hawaii*, November 7-8, 2001.
13. Evans SM, Leksono T, McKinnel PD. Tributyltin pollution: a diminishing problem following legislation limiting the use of TBT-based anti-fouling paints. *Marine Pollution Bulletin.* 1995;30:14-21.
14. Swain G**.** Biofouling control: a critical component of drag reduction. International Symposium on Seawater Drag Reduction, The Naval Undersea Warfare Center, Newport. 1998;155-161.
15. Evans SM. TBT or not TBT?: that is the question. *Biofouling.* 1999; 14:117-129.
16. Champ MA. A review of organotin regulatory strategies, pending actions, related costs and benefits. *The Science of the Total Environment.* 2000;58:21-71.
17. Lewis PN, Riddle MJ, Hewitt CL. Management of exogenous threats to Antarctica and the sub-Antarctic Islands: balancing risks from TBT and non-indigenous marine organisms. *Marine Pollution Bulletin*. 2004;45:999-1005.
18. Anderson C, Atlar M, Callow M, Candries M, Milne A, Townsin RL. The development of foul-release coatings for seagoing vessels. *Journal of Marine Design and Operations.* 2003;December:11-23.
19. Rittschof D. Natural product antifoulants and coatings development. In: *Marine Chemical Ecology*. McClintock JB, Baker BJ. Boca Raton: CRC Press; 2001:543-557.
20. Clare AS, Rittschof D, Gerhart DJ, Maki JS. Molecular approaches to non-toxic antifouling. *Invertebrate Reproduction and Development.* 1992;22:67-76.
21. Clare AS. Towards non-toxic antifouling. *Journal of Marine Biotechnology.* 1998;6:3-6.
22. Kiil S, Dam-Johansen K, Weinell CE, Pedersen MS. Sea water-soluble pigments and their potential use in self-polishing antifouling paints: simulation-based screening tool. *Progress in Organic Coatings.* 2002; 45:421-432.
23. Shilton C. Mechanism of action of tin-free antifouling paints Intersmooth 360 Ecoloflex. *Pitture e Vernici Europe.* 1997;73:10-18.
24. Konstantinou IK, Albanis TA. Worldwide occurrence and effects of antifouling paint co-biocides in the aquatic environment: a review. *Environment International.* 2004;30:235-248.
25. van Wezel AP, van Vlaardingen P. Environmental risk limits for antifouling substances. *Aquatic Toxicology.* 2004;66:427-444.
26. Voulvoulis N, Scrimshaw MD, Lester JN. Alternative antifouling biocides. *Applied Organometallic Chemistry.* 1999;13:135-143.
27. Katranitsas A, Castritsi-Catharios J, Persoone G. The effects of copper-based antifouling paint on mortality and enzymatic activity of a non-target marine organism. *Marine Pollution Bulletin.* 2003;46:1491-1494.
28. Kiil S, Weinell CE, Pedersen MS, Dam-Johansen K. Analysis of self-polishing antifouling paints using rotary experiments and mathematical modelling. *Ind Eng Chem Res.* 2001;40:3906-3920. Supplementary information available in http://pubs.acs.org.
29. Kiil S, Weinell CE, Pedersen MS, Dam-Johansen K. Mathematical modelling of a self-polishing antifouling paint exposed to sea water: a parameter study. *Chem Eng Res Des.* 2002;80:45-52.
30. Kiil S, Weinell CE, Pedersen MS, Dam-Johansen K, Arias Codolar S. Dynamic simulations of a self-polishing antifouling paint exposed to sea water. *J Coat Tech*. 2002;74:45-54. Due to a misprint, figure corrections were provided in *J Coat Tech*. 74:89-91.
31. Kiil S, Dam-Johansen K, Weinell CE, Pedersen MS, Arias Codolar S. Estimation of polishing and leaching behaviour of antifouling paints using mathematical modelling: a literature review. *Biofouling.* 2003; 19(Supplement):37-43.
32. Yebra DM, Kiil S, Weinell CE, Dam-Johansen K. Parametric study of tin-free antifouling model paint performance using rotary experiments. Accepted for publication by *Industrial and Engineering Chemistry Research*. 2005.
33. Yebra DM, Kiil S, Weinell CE, Dam-Johansen K. Reaction rate estimation of controlled-release antifouling paint binders: rosin-based systems. *Progress in Organic Coatings.* 2005;53:256-275.
34. Yebra DM, Kiil S, Weinell CE, Dam-Johansen K. Presence and effects of marine microbial biofilms on biocide-based antifouling paints. Accepted for publication in *Biofouling*. 2006;22 (1/2).
35. Yebra DM, Kiil S, Weinell CE, Dam-Johansen K. Effects of marine microbial biofilms on the release rate of biocides from chemically active antifouling paints: a model-based analysis. Submitted for publication to *Progress in Organic Coatings.*
36. Ferry JD, Carritt DE. Action of antifouling paints. Solubility and rate of solution of cuprous oxide in sea water. *Industrial and Engineering Chemistry.* 1946;38:612-617.
37. Marson F. Anti-fouling paints I. Theoretical approach to leaching of soluble pigments from insoluble paint vehicles. *J Appl Chem.* 1969; 19:93-99.
38. Yebra DM, Kiil S, Weinell CE, Dam-Johansen K. Dissolution rate measurements of sea water soluble pigments for antifouling paints: ZnO. Submitted for publication to *Progress in Organic Coatings*.
39. de la Court FH, de Vries HJ. The leaching mechanism of cuprous oxide from antifouling paints. *Journal of the Oil and Colour Chemists' Association.* 1973;56:388-395.
40. Caprari JJ, Meda JF, Damia MP, Slutzky O. A mathematical model for leaching in insoluble matrix films. *Industrial and Engineering Chemistry Research.* 1990;29:2129-2133.
41. Conference Proceedings. Protecting the ship while safeguarding the environment; London. 5-6 April 1995, Society of Wetland Scientists, KS, 1-12.
42. Vallée-Rehel K, Mariette B, Hoarau PA, Guerin P. Etude par coulométrie de la penetration de l'eau dans des films de Polymères Formulés. Analusis. 1998;26:1-7. In French.
43. Abd El-Malek MM, Mohsen RM, Ayoub MMH. New approach to the effect of binder composition on antifouling efficiency using scanning electron microscopy. *Journal of the Oil and Colour Chemists' Association.* 1997;11:337-341.
44. Sharma VK, Millero FJ. The oxidation of Cu(I) in electrolyte solutions. *Journal of Solution Chemistry.* 1988;17:581-599.
45. Kester DR. Chemistry of iron in marine systems. *Naval Research Reviews.* 1974;27:1-16.
46. Wiesenburg DA, Little BA. A synopsis of the chemical/physical properties of sea water. *Ocean Physics and Engineering.* 1987. 1988; 12:127-165.
47. Wakao N, Smith JM. Diffusion in catalyst pellets. *Chemical Engineering Science.* 1962;17:825.
48. Yebra DM. Efficient and environmentally friendly antifouling paints. Ph.D. Thesis, Technical University of Denmark, 2005.
49. Bhatia SK, Perlmutter DD. A random pore model for fluid-solid reactions: I. Isothermal, kinetic control. *AIChE Journal.* 1980;26:379-386.
50. Gupta JS, Bhatia SK. A modified discrete random pore model allowing for different initial surface reactivity. *Carbon.* 2000;38:47-58.
51. Bhatia SK, Gupta JS. Mathematical modelling of gas-solid reactions. *Reviews in Chemical Engineering.* 1992;8:177-258.
52. Villadsen J, Michelsen ML. *Solution of Differential Equation Models by Polynomial Approximation*. Englewood Cliffs: Prentice-Hall; 1978.
53. Zhang Y, Cao Z, Yang X, Yao G. The solubility of poorly soluble electrolytes in complex solutions. *Hydrometallurgy.* 1998;50:103-110.
54. Preis W, Gamsjäger H. Thermodynamic investigation of phase equilibria in metal carbonate-water-carbon dioxide systems. *Monatshefte für Chemie.* 2001;132:1327-1346.
55. Haslbeck E. Holm ER. Tests on leading rates from antifouling coatings reveal high level of variation in results among laboratories. *European Coatings J*. 2005;10:26-31.
56. Thomsen K, Rasmussen P. Modelling of vapor-liquid-solid equilibrium in gas-aqueous electrolyte systems. *Chemical Engineering Science.* 1999;54:1787-1802.

*Manuscript received Aug. 2, 2005, and revision received Dec. 14, 2005.*